

# Object-based mapping of shallow marine habitats using Sentinel-2A images on Rakit Island, Sumbawa Regency, West Nusa Tenggara

Ananda Satria Maulana<sup>1</sup>, Syamsul Bahri Agus<sup>2\*</sup>, James Parlindungan Panjaitan<sup>2</sup> and Taslim Arifin<sup>3</sup>

<sup>1</sup>Marine Technology Study Program, Department of Marine Science and Technology, Faculty of Fisheries and Marine Science, IPB University, Bogor, 16680, Indonesia

<sup>2</sup>Department of Marine Science and Technology, Faculty of Fisheries and Marine Science, IPB University, Bogor, 16680, Indonesia

<sup>3</sup>National Research and Innovation Agency (BRIN), KST Soekarno, Cibinong, Bogor, 16911, Indonesia

**Abstract.** Rakit Island in Saleh Bay, West Nusa Tenggara, possesses shallow marine ecosystems that are ecologically important but remain under-studied. This study aimed to map shallow marine benthic habitats in the waters of Rakit Island using Sentinel-2A satellite imagery. An object-based image analysis (OBIA) approach combined with a Support Vector Machine (SVM) classification algorithm was applied. The methodological workflow included atmospheric correction, water column correction, multiresolution segmentation, a two-level classification process, and accuracy assessment using field validation data. The classification results identified seven benthic habitat classes, namely rocks, sand, muddy sand, seaweed, debris, live coral, and dead coral with algae. The overall classification accuracy reached 69.01%, with a kappa coefficient of 0.63, indicating a good level of agreement between the classification results and field observations. The main limitations were spectral similarity among habitat classes and the influence of water turbidity, particularly affecting seaweed detection in deeper waters. Overall, the results demonstrate that the OBIA–SVM approach is effective for mapping shallow marine habitats using medium-resolution Sentinel-2A imagery.

**Keywords:** Shallow marine habitat, OBIA, SVM, Saleh Bay

## 1 Introduction

Saleh Bay is a water body located between the Sumbawa Regency and Dompu Regency, West Nusa Tenggara Province [1]. The waters of Saleh Bay have several small islands, including the Rakit Island. Research conducted on this island, especially regarding shallow marine habitats, is still minimal, and mapping shallow marine habitats can be used as basic information for regional development so that utilization can be optimized. The waters of

---

\* Corresponding author: [sba\\_cacul@apps.ipb.ac.id](mailto:sba_cacul@apps.ipb.ac.id)

Saleh Bay have a variety of coastal and marine biological resources, as well as favourable environmental conditions, such as temperature, salinity, dissolved oxygen, current velocity, brightness, pH, and nutrient concentrations (nitrogen and phosphorus) [2]. Rakit Island was chosen as the research location because it has been minimally studied in terms of its shallow marine habitats.

Shallow marine habitats are groups of species or communities that live on the seabed and influence each other [3]. Shallow marine habitats are home to various types of organisms, including living coral, dead coral, seagrass, algae, mud, and coral fragments. Coral reef and seagrass ecosystems are important components of shallow marine waters as spawning grounds, feeding grounds, habitats for marine biota, coastal protection from waves, sediment stabilizers, water purifiers, carbon sinks, sources of industrial and pharmaceutical materials, and tourism [4]. Shallow marine habitats are potentially subject to change owing to human activities in the uncontrolled exploitation of natural resources and the occurrence of natural factors. Changes in shallow marine habitats can be monitored through spatial analysis using remote sensing technology. Remote sensing is the best approach for monitoring coastal areas and shallow marine waters over a wide area [5]. Remote sensing technology has been widely used to detect changes in shallow marine habitats owing to the availability of easily accessible data, as well as its ability to save time, energy, and cost [6].

The use of satellite imagery to map shallow marine habitats is inseparable from the process of classification and digital imagery analysis. Digital analysis of remote sensing data generally involves two approaches: pixel- and object-based. Object-based classification or Object-Based Image Analysis (OBIA) is a subfield of GIS science that focuses on developing object-based remote sensing image analysis methods to identify several objects that have certain similarities [7]. According to [8], the application of OBIA techniques for satellite image classification provides results with better accuracy than conventional pixel-based techniques. This is because OBIA is an approach in which the classification process considers not only the spectral aspects but also the spatial aspects of objects. Objects are formed through a segmentation process, which involves grouping pixels that are close together and have the same quality (spectral similarity). According to [9], classification using the OBIA method can improve the accuracy of shallow marine habitat mapping.

The OBIA method can be performed using satellite imagery, one of which is Sentinel-2A. Sentinel-2A imagery was used to determine the distribution of shallow marine habitats on Rakit Island. Sentinel-2A imagery has advantages that support the mapping of shallow marine habitats, such as a spatial resolution of 10 m in the visual and near-infrared bands, which is sufficient for shallow water [10]. Another advantage is that Sentinel-2A data are available free of charge and have wide coverage, as well as a high recording frequency with a temporal resolution of 5 days, making it easy to obtain the latest data and select good cloud cover [4]. This study not only produced a map of shallow marine habitat classification but also analyzed the accuracy level of the classification results to ensure data validity.

## **2 Method**

### **2.1 Location and ata**

The research was divided into three stages: data collection, processing, and analysis. Data were collected in April 2025 in the waters of Rakit Island, Sumbawa, and West Nusa Tenggara. Data analysis and interpretation were performed at the Spatial Mapping and Modeling Laboratory, Department of Marine Science and Technology, Faculty of Fisheries and Marine Science, IPB University. The research location map is shown in **Fig. 1**.

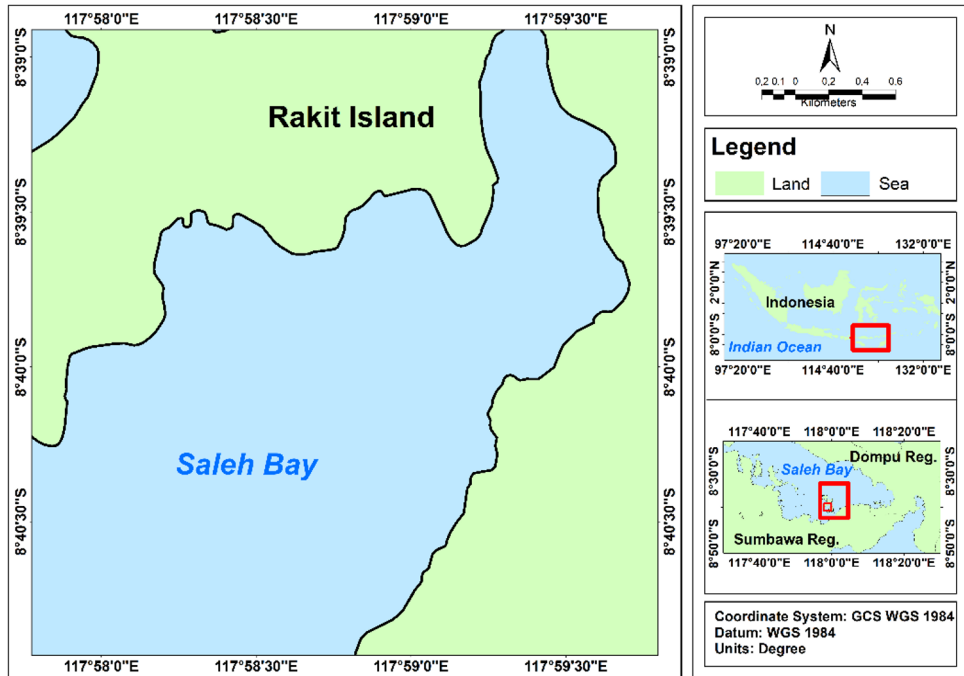


**Fig. 1.** Map of the research location on Rakit Island, Saleh Bay, Sumbawa Regency, West Nusa Tenggara, Indonesia. This map illustrates the geographical position of the study area used for shallow marine habitat mapping.

## 2.2 Data acquisition

Field observations were conducted to prepare for data collection, namely, the collection of shallow marine habitat coordinates and field documentation. Data collection on shallow marine habitats was conducted using a simple random sampling method with square transects ( $1 \times 1$  m). The coordinates of each transect point were recorded using an Olympus Tough TG 8, which contained a Global Positioning System (GPS). There were 239 shallow marine habitat sampling points that were divided into two functions: 168 points were used for classification and 71 points were used for accuracy testing. The sampling points for the shallow marine habitats in the field are shown in **Fig. 2**.

The tools used in this study consisted of several devices to support data collection and processing, both in the field and laboratory. An Olympus Tough TG-8 camera was used for the visual documentation of shallow marine habitats. Smartphones are used as tools for data recording and navigation in the field. Basic diving equipment was used to support direct underwater observations, such as visual observations that could not be observed from the sea surface. A  $1 \times 1$  m transect was used to limit the observation area so that data collection could be conducted in a measurable and consistent manner between locations. Newtop paper was used as a manual recording medium in the field to record shallow marine habitat data and other field notes that supported the spatial analysis.

Data processing and analysis were performed using a laptop with 8 GB of RAM, which is sufficient for image processing applications. The software used included ArcMap 10.8 for vector and raster-based spatial data visualization, ENVI 5.3 for multispectral image processing and analysis, and QGIS as an open-source alternative that supports spatial data processing. In addition, eCognition Developer 64 was used to perform object-based

segmentation (OBIA) as the core of the habitat classification process, while Microsoft Excel and Microsoft Word were used for tabular data processing, accuracy calculations, and thesis preparation.

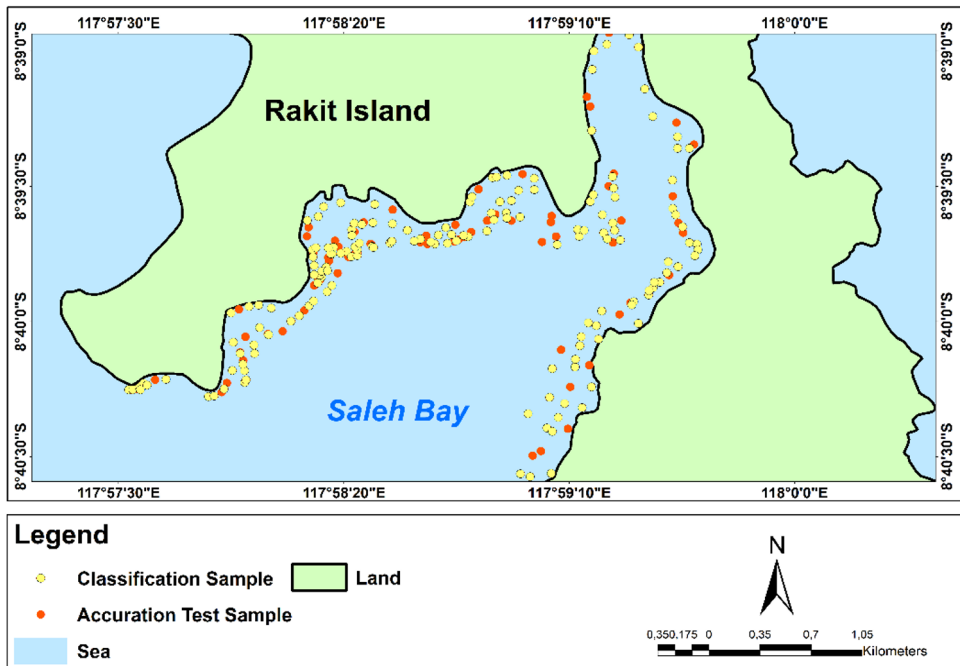


**Fig. 2.** Map showing the distribution of shallow marine habitat sampling points in the waters of Rakit Island. These sampling points were used as reference data for habitat classification and accuracy assessment of the Sentinel-2A image analysis.

The main material used in this study was Sentinel-2A satellite imagery of the Rakit Island region, which serves as the main data source for mapping shallow marine habitats. The coordinates obtained from the field surveys were used as reference data for the classification process and as training data input in the object-based classification algorithm. Sentinel-2A images were obtained free of charge from the official website of the European Space Agency (ESA; <https://dataspace.copernicus.eu>). The technical specifications of the Sentinel-2A images used in this study are listed in **Table 1**.

The research procedure began with the collection of primary data through field surveys, which included determining sample points and shallow marine habitat accuracy points as well as filling out field data sheets (HPLD data sheets). Sentinel-2A satellite images were downloaded from the official Copernicus Open Access website and underwent preprocessing including atmospheric correction and water column correction.

The next step was image segmentation using a multiresolution segmentation method to produce homogeneous objects, which were used for the analysis. The segmentation results were then classified using a support vector machine (SVM) algorithm based on training data from the field. This classification produced a map of the shallow marine habitat distribution in the study area. The accuracy of the classification results was obtained by conducting an accuracy test using field reference point data. If the accuracy was too small or too large, the segmentation process was repeated.

**Table 1.** Technical specifications of Sentinel-2A satellite imagery used in this study. This table provides detailed information on spectral bands, wavelengths, and spatial resolution of the imagery (dataspace.copernicus.eu).

Band	Band name	Wavelength (nm)	Spatial resolution (meters)
1	Coastal aerosol	433 - 453	60
2	Blue	457 – 522	10
3	Green	542 – 577	10
4	Red	650 – 680	10
5	Red Edge 1	697 – 712	20
6	Red Edge 2	727 – 752	20
7	Red Edge 3	773 – 793	20
8	Near Infrared (NIR)	784 – 899	10
8A	Narrow NIR	855 – 875	20
9	Water vapor	935 - 955	60
10	Cirrus	1,360 – 1,380	60
11	SWIR 1	1,565 – 1,655	20
12	SWIR 2	2,110 – 2,290	20

## 3 Data analysis

### 3.1 Preprocessing image

Preprocessing is an important initial stage in satellite image processing, especially in the study of shallow marine habitats. This stage aims to improve the image quality while minimizing interference (noise), which can hinder the accuracy of the spatial analysis in the next stage. The preprocessing stage begins by cropping the image area according to the study area boundaries so that the analysis focuses only on the relevant area [6].

The composite process combines several spectral channels (bands), which are important for characterizing shallow marine habitats. The composite bands used in Sentinel-2A imagery were red (B4), green (B3), blue (B2), and near-infrared (NIR) (B8). The blue and green bands have better penetration into the water column, making them very useful for detecting subsurface features such as substrates and seagrass. The red and NIR bands provide additional information related to the classification of vegetation cover in coastal areas [11]. The RGB-NIR composite provided a more complete spectral picture of shallow marine habitats. Image preprocessing produces images that are ready for use in further analyses, such as shallow marine habitat classification [12].

Atmospheric correction was performed using the Dark Object Subtraction (DOS) method, which aims to eliminate the effects of atmospheric scattering and absorption on satellite images. This process converts raw digital number (DN) values into more accurate surface reflectance values so that the resulting images can represent actual conditions in the field [13]. This correction was performed to minimize distortion due to atmospheric scattering, thereby improving the quality of spectral analysis in the next stage, particularly in mapping and classifying shallow marine habitats. The DOS method was chosen for its effectiveness and simplicity in estimating atmospheric offset values using natural dark objects as a reference [14].

### 3.2 Water column correction

Water column correction is an important step in satellite image processing in shallow marine habitat studies. The main purpose of this process is to improve the visual quality of the images by reducing the effects of light absorption and scattering that occur in the water column,

especially at certain depths. These effects can cause shallow marine habitats such as sandy substrates, seagrass, or coral reefs to become less visible, thereby hindering interpretation and classification [11]. The correction in this study was applied to Sentinel 2A images obtained on May 8, 2025, with the recording time of the satellite at 15:01 WIB, which was the time of high tide in the Rakit Island area. High tides can make underwater objects difficult to see because of the increased depth [15].

One method commonly used to correct for the influence of water columns on satellite imagery is the depth-invariant index (DII) developed by Lyzenga (1981). This method removes the water depth component from the reflectance values of multispectral imagery by comparing the logarithms of the reflectance of two different bands, namely the green and blue bands. The calculations can be performed using the following equation:

$$Y = \ln(Li) - \left[ \left( \frac{ki}{kj} \right) \times \ln(Lj) \right] \quad (1)$$

Explanation:

$Y$  = result of Invariance Depth Index transformation

$Li$  = blue band reflectance value

$Lj$  = e green band reflectance value

$Ki/kj$  = ratio of blue and green band attenuation coefficients

The  $ki/kj$  value is obtained through the following equation:

$$\frac{ki}{kj} = a + \sqrt{a^2 + 1} \quad (2)$$

$$a = \frac{(\sigma_{ii} - \sigma_{jj})}{(2\sigma_{ij})} \quad (3)$$

Explanation:

$a$  = attenuation coefficient.

$\sigma_{ii}$  = variance or variation in band i

$\sigma_{jj}$  = variance or variation in band j

$\sigma_{ij}$  = covariance of bands i and j

### 3.3 Segmentation

Segmentation is the process of grouping the pixels in an image into several homogeneous segments that represent objects with similar characteristics. The algorithm used in this study is multiresolution segmentation (MRS), which relies on three main parameters—scale, shape, and compactness—with varying values to obtain optimal segmentation results in the classification of shallow marine habitats. This algorithm starts the segmentation from a single pixel and gradually combines several segments until it reaches a predetermined heterogeneity limit. Segmentation parameter adjustments are made to avoid oversegmentation, which occurs when an object is divided into several segments, and undersegmentation, which occurs when a single segment covers more than one object. The multiresolution segmentation approach was applied at two levels: at the first level (reef level), segmentation focused on distinguishing between land, shallow waters, and deep waters; while at the second level (benthic level), segmentation was used to identify the distribution of benthic habitats in the [16]. The parameter settings used in the segmentation process are presented in **Table 2**.

The selection of scale parameter values at each segmentation level was performed through a trial-and-error approach, considering the level of visual heterogeneity, spatial boundaries of objects, and classification objectives at each level. At segmentation level 1, a scale parameter of 50 was used to produce segments sufficiently large to facilitate the separation between land, shallow sea, and deep sea classes, which have clear spectral differences.

Meanwhile, in level 2 segmentation, a smaller scale parameter of 10 was used because more detailed segmentation was needed to distinguish benthic objects, such as coral, sand, rubble, and seagrass, which are small in size and have spectral similarities between classes [17].

**Table 2.** Multiresolution segmentation parameters applied to Sentinel-2A imagery. This table summarizes the segmentation settings used at each classification level.

Level	Class	Parameters
1	Land, shallow sea, deep sea	Scale parameter = 50 Shape = 0.1 Compact = 0.5
2	Coral reefs, rubble, sand, muddy sand, rocks, seagrass, dead coral reefs with algae	Scale Parameter = 10 Shape = 0.1 Compact = 0.5

The use of lower scale values at the benthic level also aims to avoid combining different objects in one segment owing to the low spectral differences between benthic habitats. Scale parameter values are adjusted as required so that object details and generalizations are in accordance with the segmentation level used [9].

### 3.4 2-Level classification

Image classification within the OBIA framework is an advanced stage following segmentation, in which images that have been divided into several segments are further analyzed to determine object classes. At the first level, classification is performed using the contextual editing method, while at the second level, machine learning algorithms are applied to improve classification accuracy. Machine learning algorithms are mathematical approaches that utilize data for learning and produce accurate predictions or decisions [18]. The OBIA method divides images into groups of pixels that are adjacent to uniform spectral values, so that these groups can become the basic units in classification analysis [19].

Classification at each object level was performed using algorithms available in object-based image processing software, and these algorithms were combined into a set of rules tailored to specific needs. This set of rules is an integration of several algorithms used to define object classes in a structured classification process that is easy to understand through a process tree diagram. At the first level (reef level), classification is performed by setting a threshold value to determine the object class, whereas at the second level (benthic level), the SVM algorithm is used for a more detailed classification. The classification scheme for shallow marine habitats is shown in Fig 3.

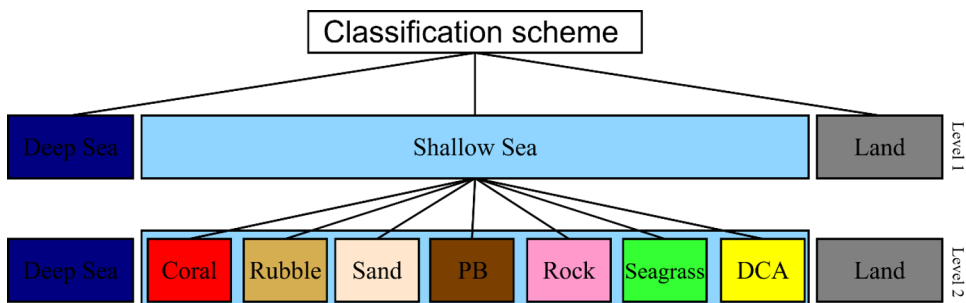


**Fig. 3.** Classification scheme of shallow marine habitats used in this study. This scheme describes the hierarchical classification structure applied in the object-based image analysis process.

The SVM algorithm works by searching for an optimal hyperplane that can effectively separate two classes of objects using a training dataset consisting of positive and negative data. The SVM training process attempts to maximize the margin, which is the distance between the hyperplane and nearest data points of each class, and minimizes the classification error rate that may occur during the training process. The SVM algorithm has the following equation [20].

$$f(x) = \sum_{i \in S} \lambda_i y_i K(x, x_i) + w_0 \quad (4)$$

Explanation:

- $K$  = kernel function
- $y_i$  and  $x_i$  = represents the training sample
- $\lambda_i$  = Lagrange multipliers
- $S$  = samples corresponding to non-zero Lagrange multipliers
- $w_0$  = hyperplane parameter

### 3.5 Accuracy test

Accuracy testing was conducted to evaluate the results of the SVM algorithm used in the classification process and assess the accuracy of the shallow marine habitat mapping results. This stage is important to ensure that the classification results spatially represent the actual conditions in the field. Accuracy testing is the basis for determining the success rate of SVM in shallow marine habitat studies. The method used to measure the accuracy is the confusion matrix.

Through this matrix, several important parameters were obtained, such as overall accuracy (OA), user accuracy (UA), producer accuracy (PA), and kappa coefficient [15]. The overall accuracy is the percentage of pixels that are correctly classified in all classes compared with the total number of accuracy test samples [21]. Producer accuracy shows the likelihood that a classified class corresponds to the field conditions or can be interpreted as accurate from the map maker's perspective. User accuracy indicates the probability that pixels classified into a class truly represent that class in the field, thus reflecting accuracy from the perspective of the map user [22]. The accuracy calculations can be explained using the following equation:

$$\text{Producer accuracy} = \frac{n_{jj}}{n_{+j}} \times 100\% \quad (5)$$

$$\text{User accuracy} = \frac{n_{ii}}{n_{i+}} \times 100\% \quad (6)$$

$$\text{Overall accuracy} = \frac{\sum_{i=1}^k n_{ii}}{n} \times 100\% \quad (7)$$

Explanation:

- $K$  = number of rows in the matrix
- $n$  = number of observations
- $n_{ii}$  = number of observations in columns  $i$  and  $i$
- $n_{jj}$  = number of observations in columns  $k$  and  $j$
- $n_{+i}$  = total marginal row  $i$ ,
- $n_{+j}$  = column total

According to [46], the kappa coefficient is a statistical indicator used to measure the level of agreement or compatibility between the classification results and the reference data used as a benchmark. This value not only shows the extent to which the two datasets match, but also considers the possibility of coincidental matches, thus providing a more objective picture than simply the accuracy percentage. The higher the kappa coefficient value, the stronger the

relationship or compatibility between the classification results and reference data. A low kappa coefficient indicates that the classification accuracy is close to random or has a weak level of agreement. The kappa coefficient value ranges from 0 to 1.00, with value categories referring to [46], as shown in **Table 3**. The equation and range of kappa coefficient values can be expressed as follows:

$$K = \frac{\sum_{i=1}^k n_{ii} - \sum_{i=1}^k n_{i+} n_{+i}}{n^2 - \sum_{i=1}^k n_{i+} n_{+i}} \tag{8}$$

Explanation:

$K$  = kappa coefficient

$n$  = number of observations

$k$  = number of rows in the matrix

$n_{ii}$  = number of observations in columns  $i$  and  $i$

$n_{+i}$  = total margin of column  $i$ .

$n_{i+}$  = total margin of row  $i$ .

**Table 3.** Kappa coefficient index and corresponding classification accuracy categories. This table was used to interpret the agreement level between classification results and reference data.

Kappa coefficient index	Category
< 0.40	Poor
0.40 – 0.60	Fair
0.60 – 0.75	Good
> 0.75	Very Good

## 4 Results and Discussion

### 4.1 Overview of the Rakit Island Region

The primary data collection site was located on Rakit Island, Labuhan Badas Subdistrict, Sumbawa Regency, and West Nusa Tenggara Province. Rakit Island is a small island in the Saleh Bay archipelago and is known for its rich marine biodiversity and significant potential for fisheries and marine ecotourism [23]. Rakit Island is not permanently inhabited, but is often used by fishermen and is an important location for coastal ecology and shallow marine research. The island is located in the southeastern part of Saleh Bay, close to the mainland of the Sumbawa Regency in the south, making it an integral part of the unique coastal and shallow marine ecological system in the West Nusa Tenggara region [24].

### 4.2 Sentinel 2A Satellite Image Correction

Atmospheric correction is an important process in satellite image preprocessing that aims to eliminate the effects of atmospheric disturbances such as water vapor, dust particles, and gas molecules, which can affect the reflectance values of surfaces that absorb or scatter electromagnetic radiation before they reach the sensor [14]. If correction is not performed, the resulting reflectance values will not accurately represent the surface conditions of the Earth, thereby reducing the data quality [25]. The differences between the satellite images before and after correction are shown in **Fig. 4**.

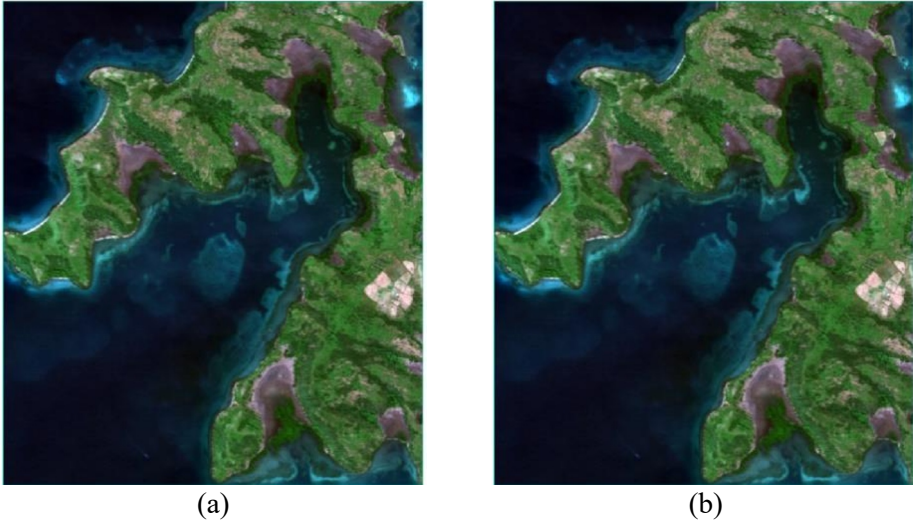


**Fig. 4.** (a) Image display before atmospheric correction (b) Image display after atmospheric correction. This figure demonstrates the visual improvement in image quality resulting from the atmospheric correction process.

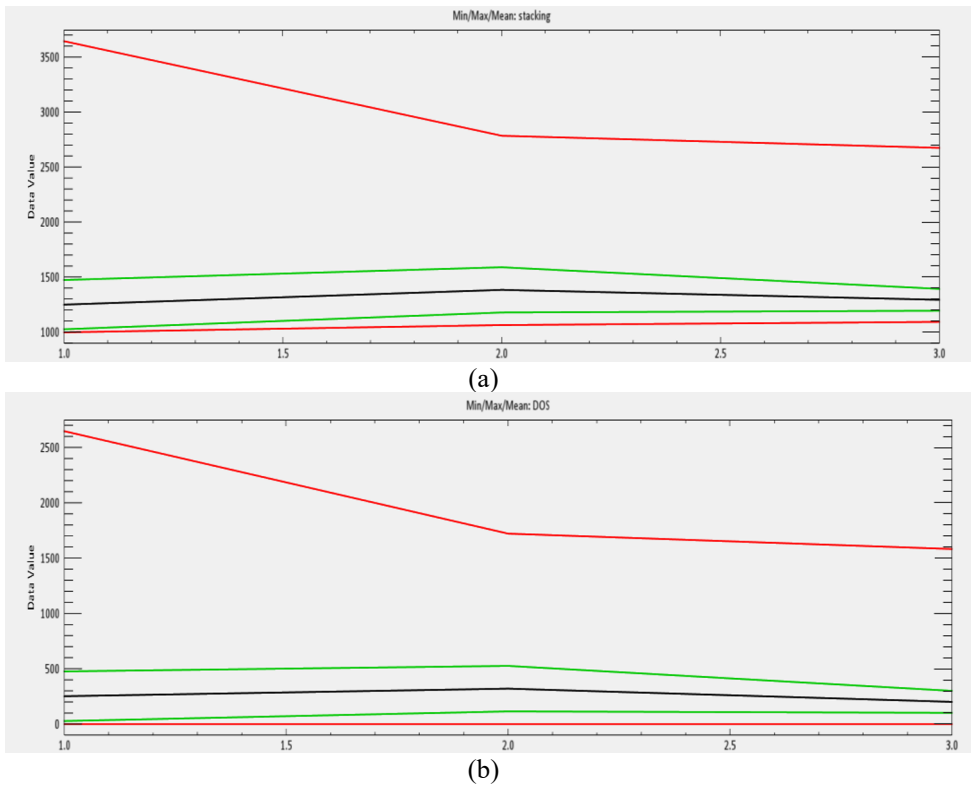


**Fig. 5.** Image (a) Histogram display before atmospheric correction (b) Histogram display after atmospheric correction. The histogram illustrates changes in reflectance value distribution after atmospheric correction was applied.

Based on the comparison of the images before and after atmospheric correction, visual differences were observed, particularly in terms of brightness and color sharpness. Atmospherically corrected images generally appeared slightly brighter, indicating that most of the dimming effects caused by the atmosphere have been corrected. This is in line with research by [14], which states that atmospheric correction significantly improves visual quality and reflectance values. The results of the atmospheric correction were analyzed quantitatively through a histogram analysis of the reflectance values of the images before and after correction. Histograms were used to show the distribution of reflectance intensity in each spectral band and to provide a more objective picture of the changes in radiometric characteristics due to atmospheric correction [45]. A comparison of the histograms is shown in **Fig. 5**.

The colored lines in the histogram represent the spectral bands of the image, namely, the red line for the red band, the green line for the green band, and the blue line for the blue band. The image histogram after atmospheric correction showed a shift in the reflectance values towards 0. This indicates that the attenuation effect caused by the atmosphere has been successfully corrected so that the reflectance values displayed are closer to the actual surface conditions [14].

### 4.3 Water Column Correction

Water column correction was applied to improve image quality by reducing the light attenuation effect caused by the water column. This correction is important because the spectral radiation from the seabed, such as sand, coral, or other shallow marine habitats, is distorted by the water column, especially at shorter wavelengths. Water column correction is applied to improve the visual and radiometric quality of images so that habitats at the bottom of shallow marine waters can be more clearly identified and distinguished [11]. Water column correction processing was carried out by calculating the attenuation coefficient ratio ( $k_i/k_j$ ) obtained from pixel value extraction in Sentinel 2A images. The resulting ratio value is 0.759714, which shows the attenuation level comparison between two wavelengths, namely, the blue and green bands. This ratio was calculated using a method based on the depth-invariant index (DII) algorithm, in which the Digital Number (DN) values of the blue and green bands were extracted from several coordinate points representing the sand substrate and then calculated manually using Microsoft Excel. The blue and green bands were used for calculation because their spectral characteristics have a greater light penetration capability than other bands, making them suitable for analyzing shallow water substrates [26]. The results for the Sentinel 2A image after water column correction are shown in **Fig. 6**.

**Fig. 6** shows a visual comparison of Sentinel-2A images before (a) and after (b) the water column correction. Visually, image (a) shows water areas with higher brightness levels because of the water column reflectance attenuation, where the spectrum of the water substrate (such as sand, seagrass, or coral) is distorted by reflections from the water surface [33].

Image (b), which has undergone water column correction, shows differences in brightness and clarity of shallow marine habitat details. The variation in reflectance values between shallow marine habitats is more apparent than in Image (a). This difference indicates that the water column correction has been successful, enabling more accurate identification of shallow marine habitats. The application of water column correction improves the quality of image interpretation for the classification of shallow marine habitats [27].

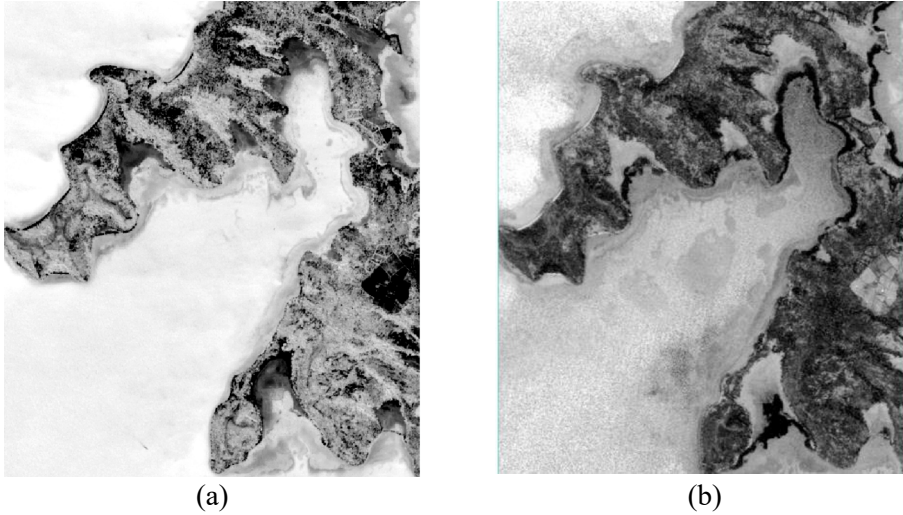


**Fig. 6.** Image Sentinel 2A image (a) before water column correction (b) after water column correction. The figures shows the effect of water column correction in enhancing the visibility of shallow marine habitats.

#### 4.4 Image Segmentation

The level 1 (coral reef level) segmentation process applied to satellite images produced three classes: land, shallow sea, and deep sea. Level 2 segmentation (benthic level) produces further segmentation results in the form of seven shallow marine habitat classes: coral reefs, debris, sand, muddy sand, rocks, seagrass, and dead coral reefs with algae. The results of the second image segmentation step continued during the classification stage. An example segmentation comparison is shown in **Fig. 7**.

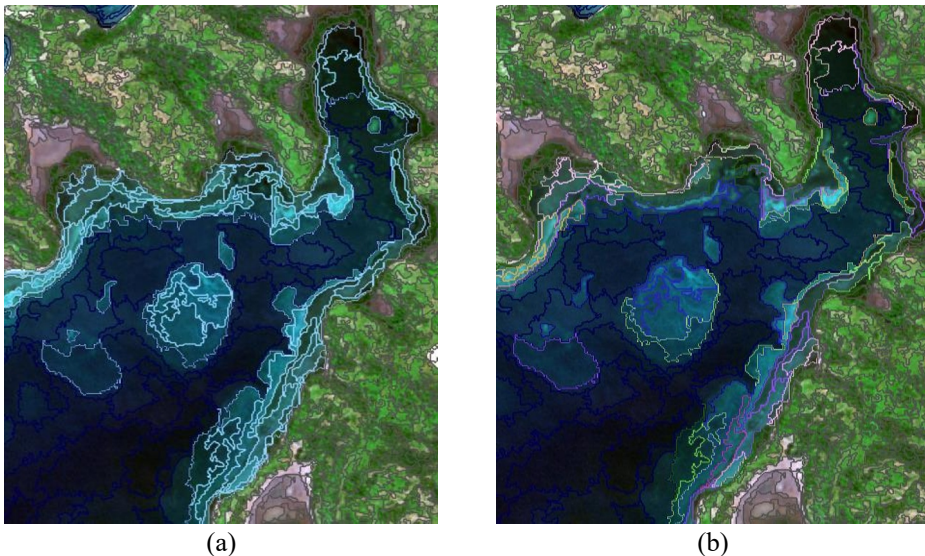


**Fig. 7.** Image Sentinel 2-A image segmentation (a) level 1 segmentation (b) level 2 segmentation. The figures illustrates the differences in segmentation scale between reef-level and benthic-level segmentation.

The satellite image segmentation process used in this study was performed to separate objects based on spectral and spatial similarities. The initial segmentation aimed to distinguish the main features in the image, namely land, shallow sea, and deep sea. These three classes were important so that the study area could become the main focus, namely, the shallow sea area, where shallow sea habitats are located. , a multi-resolution segmentation method commonly used in the OBIA approach, has proven effective in grouping pixels with similar characteristics into objects that represent habitat classes in the field [28].

Advanced segmentation steps have been specifically applied to shallow marine areas to produce more detailed classifications of shallow marine habitats. This process resulted in seven shallow marine habitat classes: coral reefs, rubble, sand, muddy sand, rocks, seagrass, and dead coral reefs overgrown with algae. More detailed segmentation was performed to distinguish between habitats that may have similar reflectance characteristics, particularly in images with medium spatial resolution, such as Sentinel-2A. The use of OBIA allows for a more accurate analysis than pixel-based approaches because it considers the spatial context and texture of objects [29].

These two segmentation results were used as the basis for benthic habitat classification. This classification process utilized the SVM machine learning algorithm, which is capable of handling the complexity of spectral data distribution from various habitat classes in the shallow seas. This visualization shows how advanced segmentation can identify and separate shallow marine habitats in greater detail and more representatively in field conditions [30].

#### 4.5 2-Level Classification Results

The classification of shallow marine habitats in this study was carried out in stages using a two-level object-based segmentation (OBIA) approach. The first stage was level 1 segmentation, which focused on reef-level classification, aiming to distinguish three main classes based on dominant spectral and spatial differences: land, shallow sea, and deep sea. This segmentation served as the initial basis for separating the target area, namely, the shallow sea zone, from non-target areas that were irrelevant for shallow marine habitat classification, such as land and deep sea. This separation is important for reducing the potential for over-classification and improving the classification accuracy in the next stage [31].

The results of the level 1 segmentation are used as a masking layer to focus the analysis on shallow sea areas, which are the inputs for the level 2 segmentation stage. At this stage, further classification was carried out on a higher scale to identify the distribution of shallow marine habitats in more detail and specificity. The classification scheme applied includes seven habitat classes: coral, dead coral with algae, debris, seagrass, sand, muddy sand, and rocks. The determination of these seven classes was based on field observations and dominant substrate characteristics in the study area. The classification results from level 1 segmentation are shown in **Fig. 8**.

The classification method used was the SVM algorithm, which is known to be effective for handling high-dimensional data and limited sample sizes [32]. In total, 168 training data points were used as representations of each habitat class, which were obtained through field verification. The classification process in the level 2 segmentation produced a map of shallow marine benthic habitat distribution with high accuracy, where each class could be spatially identified based on the spectral and texture values of the water column-corrected Sentinel-2A image [33].

The classification results from the level 2 segmentation are presented in **Fig. 9**, which shows the difference in classification detail compared to the level 1 segmentation. Level 1 segmentation serves as an initial filter that clarifies the boundaries of shallow water ecosystems, whereas level 2 segmentation provides details on shallow marine habitat classes.

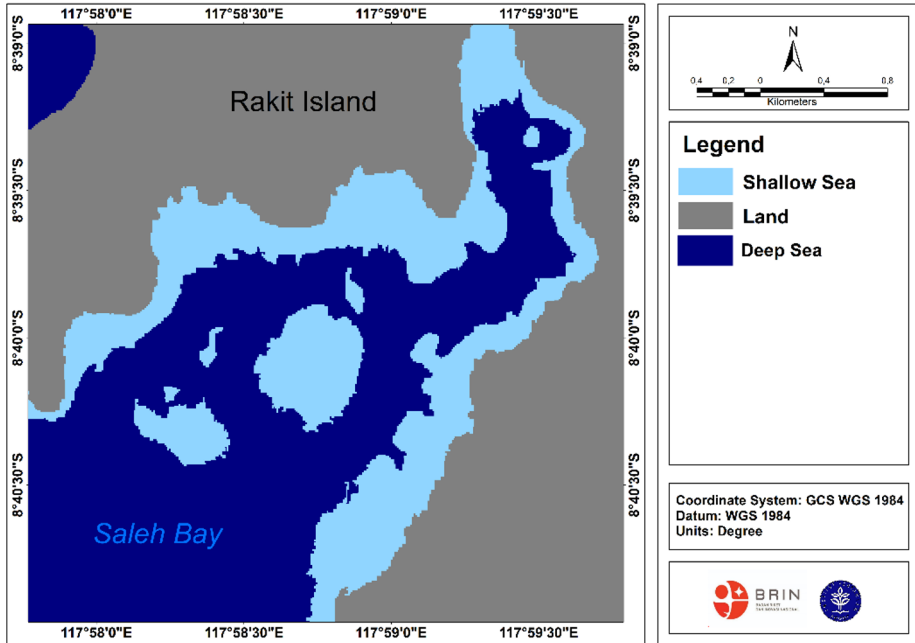


**Fig. 8.** Level 1 classification map of Sentinel-2A imagery showing land, shallow sea, and deep sea classes. This map was used as a masking layer for further benthic habitat classification.

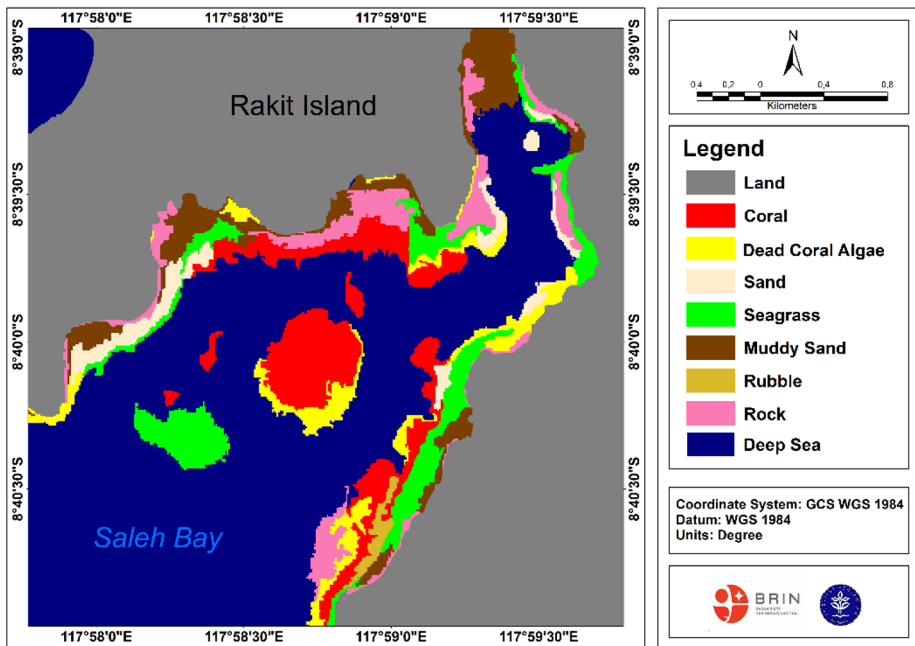


**Fig. 9.** Level 2 classification map of shallow marine habitats in the waters of Rakit Island. This map presents the spatial distribution of benthic habitat classes derived from the OBIA-SVM classification.

The shallow marine habitat classification area consists of coral, rubble, sand, muddy sand, rocks, seagrass, and dead coral with algae. The classes are listed in **Table 4**.

**Table 4.** Area coverage of shallow marine habitat classes on Rakit Island derived from Sentinel-2A imagery. This table presents the spatial extent of each habitat class based on classification results.

Class	Class area classification Sentinel 2A (ha)
Coral reef	45.1
Rubble	17.37
Sand	31.83
Muddy sand	31.50
Rock	30.88
Seagrass	50.58
Dead coral with algae	42.92

The classification of shallow marine habitats was color-coded according to the following categories: coral (red), rubble (mustard yellow), sand (beige), muddy sand (brown), rock (pink), seagrass (light green), and dead coral with algae (yellow). Based on **Table 4** and **Fig. 9**, the results of the Sentinel-2A image classification show that the shallow marine habitat on Rakit Island is dominated by seagrass ecosystems, covering an area of 50.58 ha. The dominance of seagrass reflects the characteristics of the coastal environment of Rakit Island, which supports the growth of underwater vegetation. Seagrass can grow on substrates that range from muddy to coral reefs. The substrate plays a role in determining the stability of seagrass life and as a growing medium for seagrass, so that it is not easily carried away by wave currents and as a source of nutrients. Seagrass can live and thrive on sand, sand mixed with gravel, and mud substrates with variations in morphometric characteristics related to the type of substrate and the nutrients it contains [34]. Therefore, seagrass habitats are dominant in the shallow marine waters. The living coral ecosystem covers an area of 45.18 ha, indicating that the waters around Rakit Island still have a large coral reef area. However, the area of dead coral covered with algae reached 42.92 ha, almost set, equivalent to the area of living coral. This indicates the presence of ecological pressures, such as coral bleaching due to increased water temperature, which is a direct impact of global climate change that triggers sea temperature rise and global warming. Coral bleaching occurs when seawater temperatures rise significantly, causing corals to lose the zooxanthellae that provide color and nutrients, resulting in stress and mass death of the coral ecosystem [35]. The natural process of ecological succession can also cause corals to die and become covered by algae or cyanobacteria, which eventually dominate the surface of coral substrates [36].

The rock and rubble habitats cover an area of 30.88 ha and 17.37 ha, respectively. The high percentage of rubble is caused by illegal fishing activities and sedimentation, where coral fractures cause a decline in water quality and inhibit photosynthesis of zooxanthellae living in the coral [37]. The presence of rocks at the bottom of the water reflects the morphology of the seabed, which consists of natural hard substrates around the coast of the Rakit Island. The sand and muddy sand habitats have relatively balanced areas, measuring 31.83 ha and 31.50 ha, respectively. This indicates that sedimentation processes occurred continuously in this area. Semi-enclosed waters such as Saleh Bay tend to be locations for the accumulation of sediment originating from the mainland and surrounding water activities [38].

Habitat classification is also influenced by the limited resolution of Sentinel-2A images, which have a spatial resolution of 10 m, allowing for class mixing or mixed pixels. The complexity of benthic habitats in the form of ecosystem mosaics also poses a challenge when mapping using medium-resolution satellite images, as the reflectance spectrum of some substrates, such as sand and muddy sand, is often difficult to distinguish [39, 40].

### 4.6 Accuracy test

Accuracy testing was conducted to assess the extent to which the image classification results represented the actual conditions in the field. Accuracy testing was conducted using 71 observation points from 239 available points. These points were used as validation data to compare the classification results with reference conditions. Several parameters were used to measure accuracy, namely, overall accuracy (OA), producer accuracy (PA), user accuracy (UA), and kappa value [21]. The UA, PA, OA, and kappa values for the satellite images are shown in **Table 5**.

**Table 5.** Accuracy assessment results of shallow marine habitat classification using Sentinel-2A imagery. This table summarizes the confusion matrix, overall accuracy, user accuracy, producer accuracy, and kappa coefficient.

		Sentinel 2-A Image								Total	UA (%)
		B	DCA	K	L	P	PB	R			
Field Point	B	6			2	1	2		11	54.54	
	DCA		5			2			7	71.42	
	K		1	8				1	10	80.00	
	L				8	1	2		11	72.72	
	P			1	3	9	1	1	15	60.00	
	PB	2					7		9	77.77	
	R		1	1				6	8	75.00	
Total		8	7	10	13	13	12	8	71		
PA (%)		75.00	71.42	80	61.53	69.23	58.33	75.00			
OA (%)		69.01									
Kappa		0.63									

Description: B (rock) DCA, (Dead Coral Algae), K (coral) L, (seaweed) P, (sand) PB, (Sandy Sand) R, (rubble)

Based on **Table 5**, the results of the accuracy test for shallow marine habitat classification using the SVM algorithm with Sentinel-2A imagery obtained an overall accuracy (OA) value of 69.01% and a kappa value of 0.63. This value indicates that the classification is at a moderate-to-good level of accuracy, with a sufficient level of conformity between the classification results and the actual conditions in the field [39]. According to [46], a kappa value between 0.60 and 0.75 reflects a good level of agreement in the classification of shallow marine habitats. These results indicate that Sentinel-2A imagery is suitable for the classification of shallow marine habitats in coastal areas despite its spatial resolution limitations.

The coral class shows a fairly high accuracy with producer accuracy (PA) and user accuracy (UA) of 80.00% each. This demonstrates the ability of Sentinel-2A to detect living coral reefs, even though a small portion of the coral area in the field has been classified as rubble or dead coral algae because of the spectral similarity of hard substrates in shallow marine environments [41]. In the rubble class, the classification accuracy was also quite good, with a PA and UA of 75.00%, indicating that the model was quite good at distinguishing coral fragments or other coarse substrates from other classes.

The rock class has a PA of 75.00% but a UA of only 54.54%, indicating a tendency towards over-classification in the rock class. This often occurs in rocky coastal ecosystems, where the spectral values of the rock class are difficult to distinguish from other hard substrates, such as rubble or dead coral, in multispectral images [42]. The sand class showed a PA of 69.23% and UA of 60.00%, indicating a mixture of sand with muddy sand and seagrass [42].

Seagrass beds had a PA of 61.53% and UA of 72.72%. The low PA in seagrass beds is due to the effect of seawater turbidity, which affects light penetration, making it difficult to

optimally detect seagrass spectral values in deeper waters [32]. In addition, seagrass with low density or seagrass beds mixed with sand increases the classification error rate [43]. The dead coral with algae (DCA) class has a balanced PA and UA of 71.42%, indicating a fairly good classification ability in detecting dead coral substrates that have been overgrown with algae, although there is often overlap with the rubble or live coral classes owing to spectral proximity [44].

The muddy sand class showed the lowest PA of 58.33%, although the UA reached 77.77%. This indicates that most of the muddy sand predictions on the map were consistent with field conditions, but there were areas of muddy sand that were not detected because they were classified as mixed with sand or seagrass. This phenomenon is common in benthic habitats with high sedimentation in semi-enclosed bays such as Saleh Bay [23].

## 5 Conclusion

Based on the results of shallow marine habitat mapping research using Sentinel-2A imagery on Rakit Island, habitat classification successfully identified seven main classes: coral reefs, rubble, sand, muddy sand, rocks, seagrass, and dead coral reefs overgrown with algae. The OBIA-based classification method with the SVM algorithm and multiresolution segmentation provided a fairly good level of accuracy, with an overall accuracy of 69.01% and a kappa coefficient of 0.63, which is considered good. However, each class has its own challenges, such as the difficulty of spectrally distinguishing between rocks and other hard substrates as well as the effect of water turbidity, which affects the accuracy of seagrass detection in deeper waters. Habitat classes with similar spectral values are also sources of classification errors, especially between sand, muddy sand, and seagrass.

## References

1. E. Kusumawati, S.B. Susilo, S.B. Agus, A. Taslim, Y. Yulius, Analisis penentuan sebaran konsentrasi klorofil-a dan produktivitas primer di Perairan Teluk Saleh menggunakan citra satelit Landsat OLI 8. *J. Pengelolaan Sumberdaya Alam dan Lingkungan*. **9**, 3 (2019). <https://doi.org/10.29244/jpsl.9.3.671-679>
2. Y. Yulius, M. Ramdhan, J. Prihantono, D.G. Pryambodo, D. Saepuloh, H.L. Salim, R.I. Zahara, Budi daya rumput laut dan pengelolaannya di pesisir Kabupaten Dompu, Provinsi Nusa Tenggara Barat berdasarkan analisa kesesuaian lahan dan daya dukung lingkungan. *J. Segara*. **15**, 19-30 (2019). <https://doi.org/10.15578/segara.v15i1.7429>
3. T. Blaschke, G.J. Hay, M. Kelly, S. Lang, P. Hofmann, E. Addink, D. Tiede, Geographic object-based image analysis - towards a new paradigm. *ISPRS J. of Photogrammetry and Remote Sensing*. **87**, 180-191 (2014). <https://doi.org/10.1016/j.isprsjprs.2013.09.014>
4. C.D. Prawoto, Hartono, Pemetaan habitat bentik dengan citra multispektral Sentinel-2A di Perairan Pulau Menjangan Kecil dan Menjangan Besar, Kepulauan Karimunjawa. *J. Bumi Indonesia*. **7**, 2-8 (2018)
5. Mukrimin, L.O.M. Yasir Haya, A. Takwir, Pemetaan habitat bentik perairan dangkal di pesisir Pulau Tiga (Selat Tiworo) menggunakan citra satelit Sentinel-2A. *Sapa Laut*. **6**, 63-74 (2021). <https://doi.org/10.33772/jsl.v6i1.17558>
6. A.D. Purwanto, K.T. Setiawan, Deteksi awal habitat perairan laut dangkal menggunakan teknik optimum index factor pada citra SPOT 7 dan Landsat 8. *J. Kelautan*. **12**, 2 (2019). <https://doi.org/10.21107/jk.v12i2.5400>

7. L.O.K. Mastu, B. Nababan, J.P. Panjaitan, Pemetaan habitat bentik berbasis objek menggunakan citra Sentinel-2 di perairan Pulau Wangi-Wangi Kabupaten Wakatobi.. *J. Trop. Mar. Sci. Tech.* **10**, 381-396 (2018).  
<https://doi.org/10.29244/jitkt.v10i2.21039>
8. T. Subarno, V.P. Siregar, S.B. Agus, Integration of OBIA and BTM for mapping the complexity of coral reef habitats on Harapan–Kelapa Island, Thousand Islands. *J. Coast. and Mar.* **2**, 1 (2018). <https://doi.org/10.29244/COJ.2.1.11-22>
9. A. Anggoro, V.P. Siregar, S.B. Agus, Pemetaan zona geomorfologi ekosistem terumbu karang menggunakan metode OBIA, studi kasus di Pulau Pari. *J. Penginderaan Jauh dan Pengolahan Data Citra Digital.* **12**, 1 (2015).  
<https://doi.org/10.30536/inderaja.v12i1.3306>
10. A. Rahman, V.P. Siregar, J.P. Panjaitan, Estimasi kedalaman perairan dangkal menggunakan citra satelit multispektral Sentinel-2A. *J. Segara.* **16**, 3 (2020).  
<https://doi.org/10.15578/segara.v16i3.8562>
11. A. Anggoro, D. Zamdial, D. Hartono, D. Bakhtiar, N.E. Herliany, M.A.F. Utami, Pemetaan habitat perairan dangkal menggunakan citra resolusi menengah dengan metode klasifikasi berbasis piksel (studi kasus Pulau Tikus). *J. Enggano.* **5**, 1 (2020).  
<https://doi.org/10.31186/jenggano.5.1.78-90>
12. F. Aldin, Y. Prasetyo, M. Helmi, Studi pemetaan habitat dasar perairan laut dangkal berdasarkan analisis digital menggunakan citra Pleiades multispektral di perairan Pulau Menjangan Besar, Kepulauan Karimunjawa, Jawa Tengah. *JGU.* **9**, 77 (2020).  
<https://doi.org/10.14710/jgundip.2020.26202>
13. V.P. Siregar, S.B. Agus, A. Sunuddin, T. Subarno, N.N. Aziizah, Analisis perubahan habitat dasar perairan dangkal menggunakan citra satelit resolusi 25 tinggi di Karang Lebar, Kepulauan Seribu. *JITKT.* **12**, 37-51 (2020).  
<https://doi.org/10.29244/jitkt.v12i1.25528>
14. Y. Guo, R. Deng, Y. Yan, J. Li, Z. Hua, J. Wang, Y. Tang, B. Cao, Y. Liang, Dark object subtraction atmosphere correction for water body information extraction in Zhuhai-1 hyperspectral imagery. *Egypt. J. Remote Sens. Space Sci.* **27**, 382-391 (2024). <https://doi.org/10.1016/j.ejrs.2024.04.007>
15. T.P. Ilyas, B. Nababan, H. Maduppa, D. Kushardono Pemetaan ekosistem lamun dengan dan tanpa koreksi kolom air di Perairan Pulau Pajene kang, Sulawesi Selatan. *JITKT.* **12**, 1 (2020). <http://doi.org/10.29244/jitkt.v12i1.26598>
16. R. Jiménez-Lao, M.A. Aguilar, C. Ladisa, F.J. Aguilar, A. Nemmaoui, Multiresolution segmentation for extracting plastic greenhouses from Deimos-2 imagery. *ISPRS Ann. Photogramm. Remote Sens. Spatial Inf. Sci.* **V-2-2022**, 251–258 (2022).  
<https://doi.org/10.5194/isprs-annals-V-2-2022-251-2022>
17. C. Suwanprasit, Shahnawaz, Mapping burned areas in Thailand using Sentinel-2 imagery and OBIA techniques. *Science Reports.* **14**, 9609 (2024).  
<https://doi.org/10.1038/s41598-024-60512-w>
18. H.M. Engrila, S.K. Putri, N. Arifian, Monitoring perubahan tutupan lahan dengan metode Object-Based Image Analysis (OBIA) pada citra Sentinel 2A tahun 2017–2021. *JAGAT.* **6**, 264-273 (2022)
19. E. Kurniawati, V.P. Siregar, I.W. Nurjaya, Klasifikasi habitat perairan dangkal berbasis objek menggunakan citra Worldview 2 dan Sentinel 2B di Perairan Kepulauan Seribu. *JITKT.* **12**, 421-435 (2020).  
<https://doi.org/10.29244/jitkt.v12i2.26089>

20. A. Tzotsos, A support vector machine approach for object-based image analysis, in Proceedings of the First International Conference on OBIA, Salzburg, Austria, July 4-5 2006 (2006)
21. H.A. Purba, A.P. Mulia, Penggunaan teknologi UAV pada pemetaan pantai dengan pendekatan berbasis objek geografis. *J. Syntax admiration*. **2**, 249-262 (2021). <https://doi.org/10.46799/jsa.v2i2.187>
22. F. Al Farikhi, R.W.D. Pramono, Perbandingan algoritma classification and regression tree (CART) dan random forest (RF) untuk klasifikasi penggunaan lahan pada Google Earth Engine. *Spatial: Wahana Komunikasi dan Informasi Geografi*. **23**, 2 (2023). <https://doi.org/10.21009/spatial.232.09>
23. I.N. Edrus, S. Arief, I.E. Setyawan, Kondisi kesehatan terumbu karang Teluk Saleh, Sumbawa: tinjauan aspek substrat dasar terumbu dan keanekaragaman ikan karang. *Jurnal Ilmu Kelautan dan Perikanan*. **16**, 2 (2020). <https://doi.org/10.15578/jppi.16.2.2010.147-161>
24. M.A. Rahman, R. Wulandari, Evaluasi potensi ekowisata bahari di Pulau-pulau kecil Teluk Saleh, Nusa Tenggara Barat. *Jurnal Pariwisata dan Ekonomi Kreatif*. **8**, 1 (2022)
25. E. Vermote, C. Justice, M. Claverie, B. Franch, Preliminary analysis of the performance of the Landsat 8/OLI land surface reflectance product. *Remote Sens. Environ*. **185**, 46-56 (2016). <https://doi.org/10.1016/j.rse.2016.04.008>
26. T. Subarno, V.P. Siregar, S.B. Agus, Evaluasi citra Worldview-2 untuk pendugaan kedalaman perairan dangkal Pulau Kelapa-Harapan menggunakan algoritma rasio band. *Geoplanning*. **2**, 30-37 (2015). <https://doi.org/10.14710/geoplanning.2.1.30-37>
27. D.Y. Sativa, I.G.N. Septian, F.K. Atmanegara, Benthic habitat mapping using Sentinel-2A satellite imagery in Serewe Bay. *Jurnal Biologi Tropis*. **22**, 55-61 (2022). <https://doi.org/10.29303/jbt.v22i1.3157>
28. M.A. Aguilar, F.J. Aguilar, A. García Lorca, E. Guirado, M. Betlej, P. Cichón, C. Parente, Assessment of multiresolution segmentation for extracting greenhouses from WorldView-2 imagery, in Proceedings of the XXIII ISPRS Congress, Int. Arch. Photogramm. Remote Sens. Spatial Inf. Sci, Prague, Czech Republic, July 12-19 2016 (2016), <https://doi.org/10.5194/isprsarchives-XLI-B7-145-2016>
29. P.W. Utama, V.P. Siregar, B. Nababan, Klasifikasi habitat dasar berbasis objek di perairan dangkal Karang Lebar dan Pulau Lancang. *JITKT*. **15**, 167-184 (2023). <https://doi.org/10.29244/jitkt.v15i2.36036>
30. A. Setiawan, V.P. Siregar, S.B. Susilo, A. Mardiasuti, S.B. Agus, klasifikasi habitat bentik Atol Kaledupa Taman Nasional Wakatobi dengan algoritma support vector machine. *JITKT*. **14**, 427-438 (2022). <https://doi.org/10.29244/jitkt.v14i3.35315>
31. R. Han, P. Liu, G. Wang, H. Zhang, X. Wu, Advantage of combining OBIA and classifier ensemble methods for very high-resolution satellite image classification. *J. Sensors*. **2020**, 8855509 (2020). <https://doi.org/10.1155/2020/8855509>
32. A.A. Sabilah, V.P. Siregar, M. Amran, Comparison of seagrass cover classification based-on SVM and fuzzy algorithms using multi-scale imagery in Kodingareng Lompo Island. *JITKT*. **13**, 97-112 (2021). <https://doi.org/10.29244/jitkt.v13i1.34765>
33. M.R. Nandika, A. Ulfa, A. Ibrahim, A.D. Purwanto, Assessing the shallow water habitat mapping extracted from high-resolution satellite image with multi classification algorithms. *Geomatics and Environmental Engineering*. **17**, 69-87 (2023). <https://doi.org/10.7494/geom.2023.17.2.69>

34. J.H. Sermatang, C.I. Tupan, L. Siahainenia, Morfometrik lamun *Thalassia hemprichii* berdasarkan tipe substrat di perairan Pantai Tanjung Tiram, Poka, Teluk Ambon dalam. TRITON. **17**, 77-89 (2021).  
<https://doi.org/10.30598/TRITONvol17issue2page77-89>
35. F. Muzahadah, F.E. Shafira, M. Faishal, C. Natasya, Rusaknya ekosistem terumbu karang akibat pemanasan global dalam perspektif hukum laut. Lex Suprema. **6**, 138-154 (2024). <https://doi.org/10.12345/lexsuprema.v6i1.851>
36. N.M. Setyawan, N.T. Artiningrum, Benthic and substrate category profile of coral reef in Labuan Pandan Waters, East Lombok. J. Biol. Tropis. **21**, 171-178 (2021).  
<https://doi.org/10.29303/jbt.v21i1.2448>
37. B.S. Nugroho, S.N. Dewi, Penilaian kondisi eksisting terumbu karang di Kawasan Konservasi Perairan Karang Jeruk Kabupaten Tegal. Jurnal Sosial dan Sains. **4**, 520-534 (2024). <https://doi.org/10.59188/jurnalsosains.v4i6.1393>
38. G.A. Rahmawan, W.A. Gemilang, U.J. Wisha, R. Dhiauddin, K. Ondara, Estimation of sediment distribution based on bathymetric changes (2014–2016) in inner bay of Ambon, Maluku, Indonesia. Jurnal Segara. **15**, 67-78 (2019).  
<http://dx.doi.org/10.15578/segara.v15i2.6956>
39. E. Kurniawati, D. Apdillah, J. Safitri, Pemetaan habitat bentik menggunakan citra sentinel-2a dengan algoritma maximum likelihood classification di Desa Pengudang. *Journal of Marine Research* **14**(2), 263–276 (2025).  
<https://doi.org/10.14710/jmr.v14i2.48946>
40. Risman, M. Syahdan, F. Tony, Klasifikasi substrat dasar habitat bentik menggunakan citra satelit sentinel-2 di Pulau Denawan Kabupaten Kotabaru. Jurnal Kelautan. **6**, 1 (2022). <https://doi.org/10.20527/m.v6i1.11811>
41. N. Nurdin, Supriadi, M. Lanuru, M.A. Akbar, I. Kartika, T. Komatsu, Accuracy of unsupervised classification to determine coral reef health using SPOT-6 and Sentinel-2A, in Proceedings of the GGT 2019 conference, Int. Arch. Photogramm. Remote Sens. Geoinf. Sci. Kuala Lumpur, Malaysia, October 1-3 (2019),  
<https://doi.org/10.5194/isprs-archives-XLII-4-W16-503-2019>
42. R. Hulskamp, A. Luijendijk, B. van Maren, A. Moreno-Rodenas, F. Calkoen, E. Kras, S. Aarninkhof, Global distribution and dynamics of mudflats. Nature Communications. **14**, 8259 (2023). <https://doi.org/10.1038/s41467-023-43819-6>
43. B.F.R. Davies, P. Gernez, A. Geraud, S. Oiry, P. Rosa, M.L. Zoffoli, L. Barillé, Multi- and hyperspectral classification of soft-bottom intertidal vegetation using a spectral library for coastal biodiversity remote sensing. Remote Sens. Environ. **290**, 113554 (2023). <https://doi.org/10.1016/j.rse.2023.113554>
44. B. Nababan, L.O.K. Mastu, N.H. Idris, J.P. Panjaitan, Shallow-water benthic habitat mapping using drone with object based image analyses. Remote Sens. **13**, 4452-4475 (2021). <https://doi.org/10.3390/rs13214452>
45. M.A. Amran, Fundamentals of satellite remote sensing (Nas Media Pustaka, Makassar, 2024)
46. R.G. Congalton, K. Green, Assessment of remote sensing data accuracy (CRC Press, New York, 2019)